ACS APPLIED MATERIALS & INTERFACES

Research Article

www.acsami.org

Electric Field Induced Morphological Transitions in Polyelectrolyte Multilayers

Chungyeon Cho,[†] Ju-Won Jeon,[‡] Jodie Lutkenhaus,[‡] and Nicole S. Zacharia*[,†,§]

[†]Materials Science and Engineering Program, [‡]Artie McFerrin Department of Chemical Engineering, and [§]Department of Mechanical Engineering, Texas A&M University, College Station, Texas 77843, United States

Supporting Information

ABSTRACT: In this work, the morphological transitions in weak polyelectrolyte (PE) multilayers (PEMs) assembled from linear poly(ethylene imine) (LPEI) and poly(acrylic acid) (PAA) upon application of an electric field were studied. Exposure to an electric field results in the creation of a porous structure, which can be ascribed to local changes in pH from the hydrolysis of water and subsequent structural rearrangements of the weak PE constituents. Depending on the duration of application of the field, the porous transition gradually develops into a range of structures and pore sizes. It was discovered that the morphological transition of the LbL films starts at the multilayer-electrode interface and propagates through the film. First an asymmetrical structure forms, consisting of microscaled pores near the electrode and nanoscaled pores near the surface in contact with the electrolute solution. At longer application of the field the porous structures become microscaled throughout. The results revealed in this study not only demonstrate experimental feasibility for controlling variation in pore size and porosity of multilayer films but also deepens the understanding of the mechanism of the porous transition. In addition, electrical potential is used to release small molecules from the PEMs.

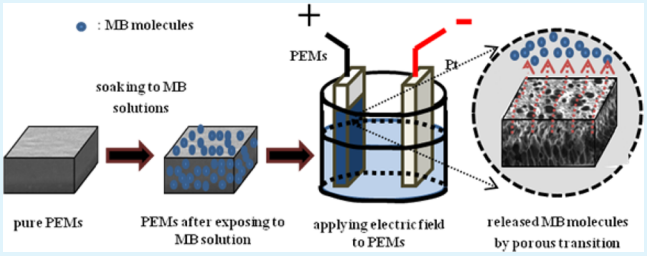

KEYWORDS: *porous structures, layer-by-layer assemblies, polyelectrolyte multilayers, electric field, small molecule release, responsive films*

INTRODUCTION

There are a number of applications for porous polymer films and coatings including cell scaffolds,[1−3] drug delivery materials,[4−6] filtration media,[7,8] separators in electrochemical devices,[9] and antireflection (AR) coatings.[10−13] The mechanical properties of cellular materials are known to vary with pore size and distribution.[14] In each case the required pore sizes and design are somewhat different. For example, cell scaffold materials need pores that are tens of micrometers large whereas AR coatings require small pores that will not scatter light. The ability to tune in pore density, size, or even pore shape or orientation would represent a breakthrough for the fabrication of materials for any of the aforementioned applications.

Polyelectrolyte multilayers (PEMs) assembled using the layer-by-layer (LbL) technique[15] are versatile films and coatings based on the directed complexation of oppositely charged polyelectrolytes (PEs), and they have been proposed for use in all of the aforementioned applications. They are typically fabricated by the sequential adsorption of oppositely charged PEs from solution onto a charged substrate. The charged functional groups of each polymer chain associate with oppositely charged groups on another chain, building up the assembly.

It has been demonstrated that porous structures can be spontaneously formed from a weak PE containing PEMs.[16,17] These films are built up at moderate pH so that the weak PEs within the film are only partially charged. When that film is exposed to a sharp change in pH, the weak PEs' functional groups become charged or charge-neutralized, ion pairs are broken and reformed, chains change conformations, and pores are formed. During this process, the thin film swells and then contracts as new ionic cross-links are formed, causing it to reject water unevenly during the contraction, which is the source of the pore formation.[18] This process is sometimes discussed as a phase separation. Stable LbL films are generally formed under conditions where the corresponding PE complex would result in a stable solid phase. Changing the charge densities of the PE changes may change this balance, creating a reorganization of the film. There is also a partial dissolution of the film during this process as a result of the phase separation. The resultant structure can be either nano- or microporous, depending on both film assembly conditions and the pH to which the film was exposed. Porosity transitions in weak PE films, including hydrogen bonded systems, induced by immersion into low-pH[19−22] or high-pH solution,[23−28] referred to as "post-assembly treatment," are well reported in the literature.[16] There have been many studies both about their fundamental nature as well as their potential applications.

Received: February 22, 2013
Accepted: May 17, 2013
Published: May 17, 2013

Recently, our group reported a method of using hydrogel stamps to deliver acid or base to a PEM in a more controlled manner,[19,26] which can result in greater control over the porous structure. In this work the weak PEs poly(acrylic acid) (PAA) and linear poly(ethylene imine) (LPEI) were used. For these PEs the charge density along the chain varies as a function of pH. In the case of PAA and LPEI the charge density follows an inverse relationship for the pair, shown in Figure 1. Our

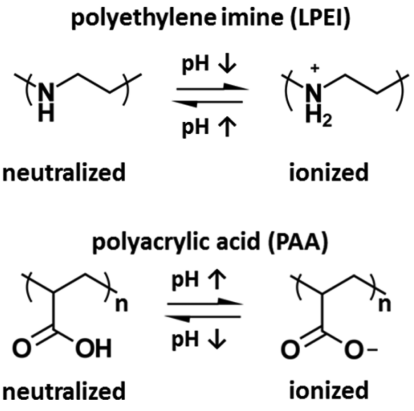

Figure 1. Molecular structures of PEs (LPEI and PAA) used in this study.

previous work also demonstrated that the change in morphology is accompanied by a loss in mass. Although the use of hydrogel stamps brings about localized control, a greater degree of temporal control may be desired, especially in a manner that could be applied to larger areas. An electric field, or the application of a controlled potential, is an extremely promising means to control the porous transition via water electrolysis, which produces a sharp change in pH, and often used to manipulate pH for responsive PE based materials.[29] The application and amplitude of the field can be controlled precisely to command precision over the transition and the resulting morphology.

Here, we demonstrate a new platform for the controlled creation of porous structures within LbL films via electric fields. Only a few methods exist to create these porous structures in a controlled way, and to our knowledge there are no reports using an electric field. Electric fields have been used to influence the assembly of PEMs but not to induce postassembly change in this manner.[30] We have applied an external electric field to the multilayers over a range of time periods. The application of an electrical potential in an aqueous solution creates protons at the electrode-LbL film interface. The protons generated locally at the electrode can be used to create the same change in film morphology from continuous to porous within the LbL films that are reported elsewhere from exposure to acidic solutions. As it is possible to carefully control the electrical field applied, it is then possible to control the formation of the porosity as well.

EXPERIMENTAL SECTION

Materials. The molecular structures of the PEs used in this study are described in Figure 1. Poly(acrylic acid) (PAA, MW = 50 000 g/mol, 25% aqueous solution) and linear poly(ethylene imine) (LPEI, MW = 40 000 g/mol) were obtained from Polysciences. Methylene blue chloride was purchased from EMD. All products were used as received without further purification. For all solutions Milli-Q 18.2 MΩ deionized (DI) water was used. All of the aqueous solutions were adjusted to the appropriate pH using 0.1 and 1 M HCl or NaOH solutions, respectively, as needed prior to multilayer assembly. Indium tin oxide-coated glass slides (ITO, Delta's Technologies) were used as substrates for the buildup of multilayers. Oxygen plasma treatment was performed to render the surface of ITO negatively charged.

PEM Formation. The LbL deposition of LPEI and PAA was achieved by alternately dipping substrates in PE solutions using a Nano Strata Sequence VI at room temperature. Each PE was used as received without further purification to create polymer solutions of 0.02 M concentration based on the repeat-unit molecular weight in Milli-Q water. Plasma-treated-ITO substrates were first immersed in the polycation (LPEI) for 15 min and rinsed in three fresh water baths for 2, 1, and 1 min. The samples were then immersed in the polyanion (PAA) for 15 min, followed again by three rinsing steps. This completed the deposition of one bilayer, which is defined as an adsorption step of polycation followed by an adsorption step of polyanion. This process was cycled until the desired number of bilayers was deposited. Unless otherwise stated, the outermost layer of the multilayers used in this experiment was the polyanion (PAA). For the remainder of this paper PEMs will be referred to as X(LPEI/PAA)$_Y$, where X is the pH value of the polycation and polyanion baths, and Y is the number of bilayers assembled. For example, 4(LPEI/PAA)$_{20}$ refers to a sample constructed from 20 bilayers of LPEI and PAA, where the pH of both baths was adjusted to 4. PEMs were dried after assembly using a stream of nitrogen gas and further dried in ambient air for several hours before the measurements.

Electrical-Field-Induced Post-Assembly Treatment. PEMs assembled on ITO substrates were used as the working electrode in a three electrode electrochemical cell. Ag/AgCl and Pt wire electrodes were used as reference and counter electrodes, respectively. The cell contained water pH-adjusted to 3.2; accordingly, the ionic strength of the Cl^- ion in pH 3.2 water was 0.59 mmol. A voltage of 4.0 V was applied for various time periods (10, 20, 30 min, and 1h), using a Solartron SI 1287 potentiostat at room temperature.

Release of Methylene Blue (MB) from LPEI/PAA Films by Applying Electrical Potential. Some LbL samples were exposed to MB solutions prior to treatment with electrical potential. LbL films assembled on ITO were immersed for 1 h into a 0.05 M MB solution containing 0.1 M NaCl at pH 7 to load MB molecules into the multilayers. Then, the loaded samples were rinsed in pH 3.2 water several times to remove physically adsorbed excess MB molecules (Supporting Information, Figure S1). The MB-loaded 4(LPEI/PAA)$_{20}$ LbL films (1.4 cm^2 in area) were then exposed to 30 mL of pH 3.2 water. An electrical potential of 4.0 V was applied for varying times, and the amount of released MB molecules into the pH 3.2 water was measured using UV−vis absorption spectra.

Characterization. Atomic force microscopy (AFM) was conducted by using a Digital Instruments Nanoscope in tapping mode (scan rate 1 Hz) under ambient conditions. The thickness of the multilayer was analyzed before and after treatment with electric field using a profilometer (KLA−Tencor Instruments P-6) with 2 μm radius stylus and 1 mg stylus force. Each sample was measured 10 times at different locations, and 5 samples of each type were measured to create statistically significant error bars. Additionally, film edges were avoided, and measurements were performed on similar portions of the films each time to both avoid defects and ensure that we were measuring similar samples. Scanning electron microscopy (SEM) images were obtained on a JEOL JSM-7500F field emission scanning electron microscope. Attenuated total reflection Fourier transform infrared spectroscopy (ATR-FTIR) spectra of PE films were collected on a Bruker Optics Alpha FT-IR spectrometer. UV−vis spectra were recorded on a Hitachi U-4100 UV−vis−NIR spectrometer.

RESULTS AND DISCUSSION

Time Evolution of Morphological Transitions. First, 4(LPEI/PAA)$_{20}$ LbL films were immersed into pH 3.2 water for 1h without any applied potential. AFM images indicate that films treated with pH 3.2 solution had a featureless and continuous surface morphology similar to the untreated films (Supporting Information, Figure S2). The RMS (root-mean-

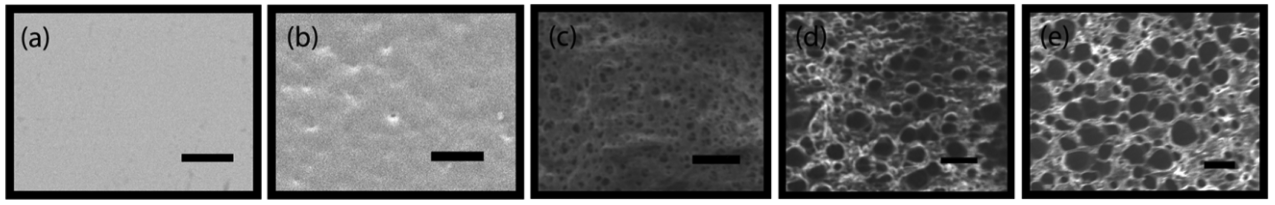

Figure 2. SEM images (top-view) of 4(LPEI/PAA)$_{20}$ LbL films after application of an electric field for various times. (a) Untreated films and those treated after (b) 10 min, (c) 20 min, (d) 30 min, and (e) 1 h of exposure to the electric field. Scale bars are 10 μm.

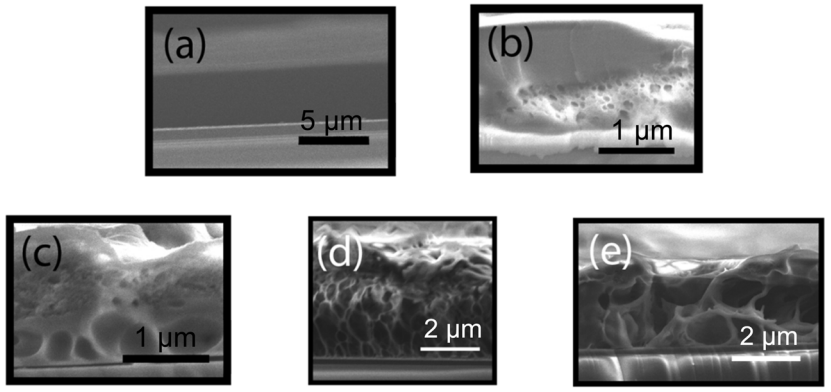

Figure 3. Cross-sectional SEM images of 4(LPEI/PAA)$_{20}$ LbL films after application of an electric field for various times. (a) Untreated films and those treated after (b) 10 min, (c) 20 min, (d) 30 min, and (e) 1 h of exposure to the electric field.

square) surface roughness of both films was also similar (1.5−2.0 nm), indicating that this pH condition has little effect on the surface morphology. However, below this pH value (pH ≤ 3.0), 4(LPEI/PAA)$_{20}$ LbL films underwent transitions in porosity, in agreement with previously reported results.

Next, we applied an electrical potential of 4.0 V vs (Ag/AgCl) to multilayer-coated ITO substrates in pH 3.2 water. Figures 2 and 3 show top-view and cross-sectional SEM images of 4(LPEI/PAA)$_{20}$ LbL films treated under electric fields for various times. The films undergo different stages of morphological evolution with characteristically different pore sizes and pore distribution with increasing time. Prior to applying the electrical potential, the thin films were relatively smooth and had a featureless morphology at the surface and in the interior. However, after 10 min of treatment, pores about 100−200 nm in size were created near the multilayer-ITO interface, while the film's surface remained smooth and intact. With increasing treatment time, the films became increasingly more opaque to the eye, while those films treated for less than 10 min were optically transparent as shown in Figure 4.

After 20 min of treatment, SEM images (Figures 2c and 3c) show a nanoporous surface and asymmetrical morphology in the interior of the film. Cross-sectional SEM images show a dense, nanoporous top layer with pores ∼100 nm in size and a microporous interior region at the film-ITO interface. At longer times (30 min), pore size and pore density increase, and the asymmetric structure remains. At 1 h of treatment the average pore size increases to several micrometers in diameter throughout the film, and the asymmetric structure vanishes.

The morphologies formed within the multilayers can be explained by considering the electrolysis of water, changes in local pH, and the breaking and reformation of ion-pair cross-links. The LbL films in this experiment were assembled using weakly charged PEs of LPEI and PAA both at pH 4, which is a pH at which both polymers are only partially charged. Both

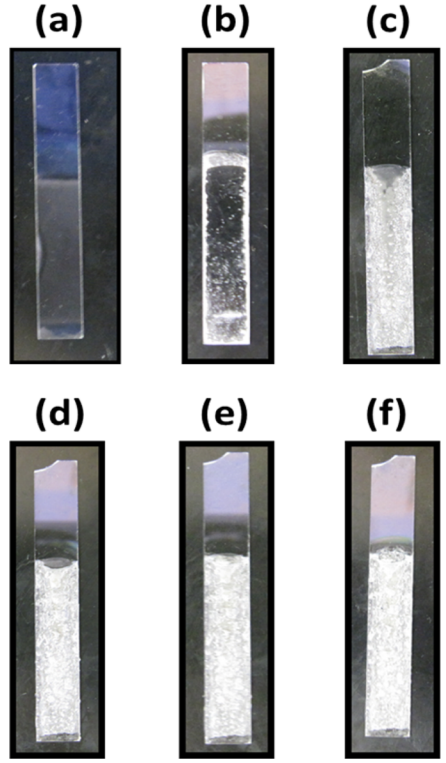

Figure 4. Optical microscopy images of 4(LPEI/PAA)$_{20}$ LbL films on ITO substrate after application of an electric field for various times. (a) Untreated films and those treated after (b) 5 min, (c) 10 min, (d) 20 min, (e) 30 min, and (f) 1 h of exposure to the electric field.

LPEI (pK_a ∼ 6) and PAA (pK_a ∼ 5.5 − 6.5)[31] chains adsorb in loop-rich conformations with an ion-paired internal structure at this pH condition. However, when an anodic electrical potential (4.0 V vs Ag/AgCl) is applied, water electrolysis occurs, and the

local pH at the film-ITO interface becomes markedly acidic by the following reaction:[32−34]

$$2H_2O \rightarrow 4H^+ + O_2 + 4e^- \quad (1)$$

Therefore, the local pH at the film-ITO interface is lower than that of the solution (pH = 3.2). Providing an exact calculation of this is challenging, however. The Henderson−Hasselbalch equation which is often used for pH calculations can only be applied to systems at equilibrium, which is not the case here. Using the Nernst equation to calculate the pH is also problematic. Although we apply 4.0 V in our experiment, much of this potential is lost to the resistance of the solution, rather than applied to the reaction in eq 1. The ionic strength is 0.59 mmol, meaning that the resistance of the solution is high. Considering that LPEI/PAA films undergo postassembly porous transitions at pH values less than 3.0, we can conclude that the local pH is less than 3.0. Thus, some of the ionic linkages between the NH_3^+ groups of LPEI layers and COO^- of PAA layers are dissociated and rearrangements of both LPEI and PAA chains lead to porosity transitions induced by the application of an electric field. A voltage of 4.0 vs (Ag/AgCl) was chosen as it represents an overpotential with respect to the hydrolysis of water and therefore the morphological transitions happen in a relatively short time frame. For comparison, we also applied 2.0 V vs (Ag/AgCl) to a film. After 3 h, no morphological changes were seen, but after 24 h, a porous morphology with large, microscaled pores was seen throughout the cross section of the film. Both optical microscopy and SEM images of the 2.0 V experiment can be seen in the Supporting Information (Figure S3 and S4, respectively).

An interesting point during the evolution of the morphological structure is the creation of an asymmetric structure with smaller pores near the free surface and larger pores near the electrode/multilayer interface. This structure is similar to those reported elsewhere both by simply immersing a PEM into an acidic solution[17] and with stamping a film to slowly release acidic solution into it.[28] However, in both of these other cases, the source of protons entering the film is from the free surface at the top of the film, whereas in the electric potential case the source is from the bottom surface of the film in contact with the electrode. At first thought, an explanation for the formation of this structure may be the diffusion of protons from the electrode through the film. Clearly, the process is diffusion mediated. In the electric field case pores are first seen at the electrode/film interface, later forming in portions of the film further away from that interface. In our previous work with stamping,[28] pores are first observed near the interface of the film and the stamp, away from the substrate. We also observe in both cases that smaller pores grow to be larger, possibly matching the formation of the asymmetric structure. However, in all three cases the same asymmetric structure is observed, larger pores at the substrate, smaller ones at the free surface, regardless of the location of the source of protons. In this work the protons are being delivered from the substrate, in the other two cases the protons are delivered from the free surface, and yet the same ultimate structure is observed.

We have considered two other possible explanations for this observation. One possibility is that the substrate somehow confines the diffusion of chains within the film and their reorganization, causing smaller pores to coalesce with one another to form larger pores. We have shown previously that loss of PE chains accompanies this morphology transformation,[28] and perhaps this is frustrated near the substrate, causing different structures to be formed.

Another possibility is that the structure of the film is different away from the substrate and near the film's top, the free interface.[35] It is generally observed that there are differences in the first few deposition steps when compared to later steps. Also, the LPEI/PAA system is one that grows exponentially;[36,37] that is, each bilayer does not have the same thickness, but during later deposit steps much more material is deposited than during earlier steps. This is attributed at least in part to the ability of one or the other of the PEs to diffuse through the growing film during deposition. It is therefore likely the case that the structure of the film is not uniform throughout. It is known both that PE charge density is extremely susceptible to the surrounding environment, and that different charge densities within weak PE films can result in different types of pores even with the same postassembly treatment.[17,28,38] We hypothesize that either the nonuniform manner of film growth for this system or some kind of confinement of the chain rearrangement and diffusion near the substrate results in the asymmetric film structure regardless of the source of protons, although the exact mechanism is not known.

Figure 5 shows the film thickness and corresponding swelling ratio for LbL films treated by electrical potential as a function of time. After the multilayers were dried under ambient conditions, the thickness measurements were performed using profilometry by analyzing 10 different regions on 5 separate samples. The thickness of each film was measured before (T_{before}) and after (T_{after}) the application of electrical potential, and the swelling percentage was calculated as $100 \times (T_{after} - T_{before})/T_{before}$.[39] After 1 h of treatment, the film thickness increased by nearly 5 times its original thickness, and the swelling percentage was calculated to be 400%, corroborating our prior SEM observations. The rms (root-mean-square) surface roughness was obtained from AFM analysis of at least 5

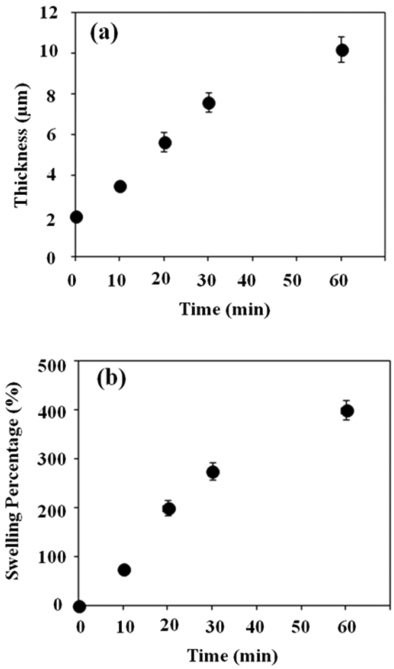

Figure 5. (a) Thickness and (b) swelling percentage of thin films after application of an electric field for various times.

separate measurements on each film (Supporting Information, Figure S5 and S6). The rms surface roughness of LPEI/PAA thin films treated after 10 min of exposure to the electric field was almost the same as that of untreated thin films, showing a continuous surface with a surface roughness of 3−4 nm. However, after 20 min of an application of electric field, the surface roughness was as high as 90 nm. With further treatment, the surface roughness increased only slightly more. As the charge density and therefore cross-link density in the film changes with application of the electric field, the osmotic pressure in the film and therefore its swelling will change because of both a change in affinity to water and the changes in cross-link density.[40] Changing charge densities will change coil conformations as well, another potential source of thickness change, and finally the introduction of pores clearly requires an increase in film thickness. Although during this process there is loss of mass, the overall percentage of film mass lost is relatively small, necessitating the increase in film thickness.

Ionization in Multilayers under an Electrical Potential. FT-IR spectroscopy of 4(LPEI/PAA)$_{20}$ LbL films was used to further investigate the influence of electrical potential on the ionization of PEs during the porous transition as a function of treatment time. Two pronounced peaks were observed at 1710 and 1550 cm^{-1} for the films, as shown in Figure 6a; the former peak is assigned to neutralized carboxylic acid groups and the latter peak corresponds to ionized carboxylate acid groups in PAA.[41,42] As the electrical potential was applied over time, the peak intensity of neutral COOH groups increased, and that of ionized COO$^-$ groups decreased. Assuming that these two absorption bands have about the same extinction coefficient,[43,44] the percentage of charged COO$^-$ groups was calculated using the ratio of the peak intensity of v(COO$^-$) to the intensity sum of v(COO$^-$) and v(COOH), Figure 6b.[31] The amount of charged COO$^-$ groups dropped from 55% to 43% in response to the application of the electrical potential for 1 h. The results of this analysis may be attributed to a change in charge density of PAA chains; upon the application of an electrical potential, partially ionized PAA become protonated because of the locally acidic environment. This result corroborates the images obtained from SEM and the observed swelling with respect to the morphological transitions after the application of electrical potential.

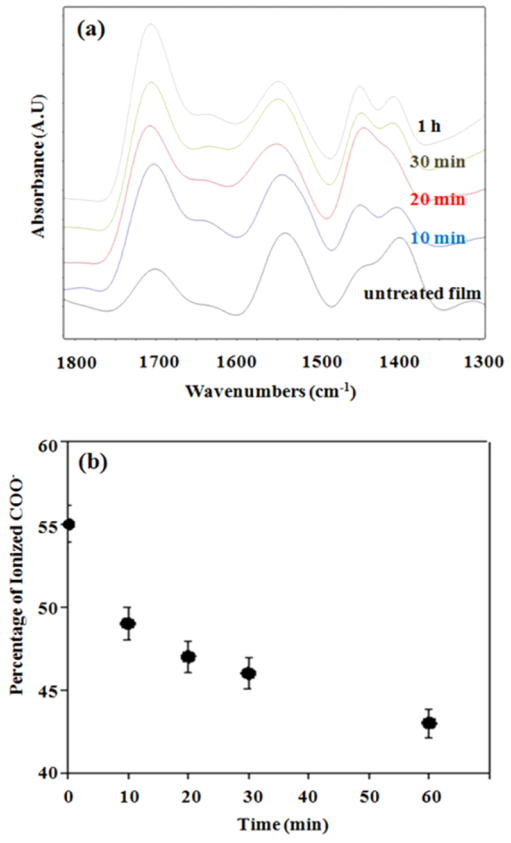

Figure 6. ATR FT-IR spectra (a) and the percentage of carboxylate group (COO$^-$) (b) of 4(LPEI/PAA) $_{20}$ films after application of an electric field for various times. The peaks of interest at 1710 and 1550 cm^{-1}, corresponding to neutralized and charged carboxylic acid groups, respectively, can be seen depending on the time period for which the electrical potential is applied.

Release of MB from the Thin Films under Electrical Potential. We also investigated the amount of MB released during the electrical potential-induced porous transition. Positively charged MB molecules bind with free, unpaired carboxylate groups, as shown in Supporting Information, Figure S1. If a carboxylate anion associated with an MB molecule becomes protonated, then the MB molecule is released. Thus, a measure of the MB released into solution using UV−vis spectroscopy should correspond to the protonation of carboxylate groups.

First, 4(LPEI/PAA)$_{20}$ LbL films were immersed into a 5 mM MB solution containing 0.1 M NaCl at pH 7 for 1 h. The UV−vis spectrum of the as-immersed film is shown in the Supporting Information, Figure S7. Peaks ranging from 500 to 750 nm are present, which indicates loading of MB into the PEMs. Pristine LbL films before loading did not show any apparent peaks in visible range. At an assembly of pH of 4.0, both LPEI (pK_a ~ 6) and PAA (pK_a ~ 5.5 − 6.5) are partially ionized. At this condition, film formation produces thick layers and loop-rich conformations; the internal structure contains a mixture of ion-paired PE and unpaired free acid and amine groups. MB is known to have its maximum absorbance peak at 664 nm,[45] but the maximum peak of 4(LPEI/PAA)$_{20}$ −MB films was observed at 585 nm with the additional shoulder peak at around 664 nm. The ~664 (n-Π*) nm band is assigned to an isolated molecule (monomer) in dilute aqueous solution,[46] and the peak at 585 nm appears when MB molecules aggregate as trimers (face-to-face association, H-aggregates).[47−51] Based on this fact, the UV−vis spectrum of thin films loaded with MB reveals that MB molecules exist as highly aggregated molecular states with the strong Π-Π interaction among MB molecules in the 4(LPEI/PAA)$_{20}$ LbL films.

Next, the MB-loaded LbL films were subjected to 4.0 V for varying times. Direct UV−vis spectroscopic measurement of the films was challenging because of the scattering of light from the porosity; therefore, UV−vis measurements were performed on the solution in the electrochemical cell to monitor the release of MB, shown in Figure 7a. As can be seen, the UV−vis solution spectra of MB released were different from the spectrum of the original MB-loaded LbL films. UV−vis spectra showed that the maximum peak was observed mainly at approximately 664 nm with a small shoulder at 615 nm, which indicates that MB molecules mainly exist as monomers and to a lesser degree as dimers when released from the multilayers into solution. As expected, the absorbance of MB released in the solution increased with the amount of time that the electrical potential was applied. These results suggest that the amount of

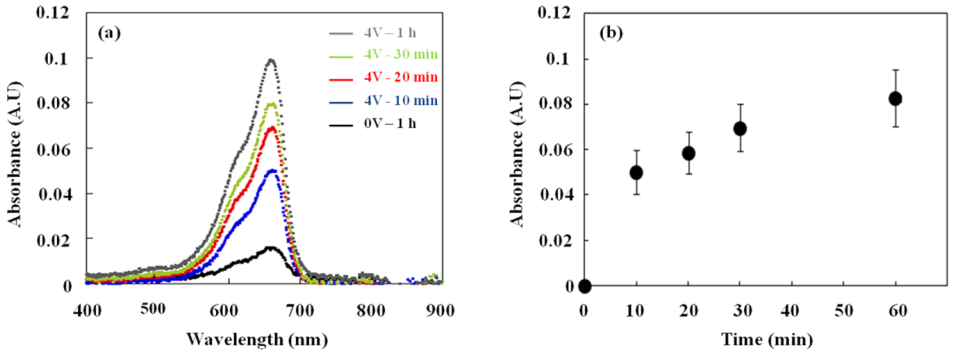

Figure 7. UV–vis spectra of released MB molecules from the 4(LPEI/PAA) $_{20}$ LbL films (a) and absorbance change (b) after application of an electric field for various times. The maximum absorbance at 664 nm of the solution in which MB-loaded LbL films were soaked with no application of electrical potential in pH 3.2 water for 1 h was 0.012. After electrical potential is applied, the maximum absorbance of the same sample increases from 0.051 at 10 min to 0.1 at 1 h treatment.

MB released can be controlled by applying an electrical potential for a certain time. As a control experiment, a MB-loaded 4(LPEI/PAA)$_{20}$ LbL film was immersed in the pH 3.2 water with no application of electrical potential for 1 h, and the UV–vis spectra of that solution was measured. Even though the peak at 664 nm corresponding to MB was observed as shown in Figure 7a, the amount of MB released passively without applying electrical potential was much smaller than those samples where an electrical potential had been applied.

The absorbance of the 664 nm peak was plotted as a function of the time that the potential was applied, shown in Figure 7b. The amount of MB released from the multilayers increases with time, coinciding with our observations of a decrease in COO^- groups from FTIR spectra and the increase in swelling percentage. It is quite evident that the amount of MB released from the films under electrical potential is directly related to the number of COOH groups remaining in the multilayers. As electrical potential is applied, COO^- groups become protonated, and fewer carboxylate groups are available for binding with the MB molecules. In addition to the protonation of COO^- groups, the nano- and microporous structures created during the application of electrical potential also expedite the diffusion of MB out of the 4(LPEI/PAA)$_{20}$ LbL films. A cursory examination of Figures 6b and 7b show that MB release seems to be an inverse function of the percentage of charged carboxylic acid groups, a relationship that is more complex than simple first order release kinetics.

Number of Protons Generated by Electrical Potential. The number of coulombs generated by the application of 4.0 V was recorded with time (Supporting Information, Figure S8). Based on the amount of coulombs produced, the number of moles of protons generated was calculated. At positive voltage (theoretically higher than 1.0 V vs Ag/AgCl),[52] water decomposes into protons and oxygen gas, and electrons are generated. While electrical potential is applied, the number of moles of protons generated is equal to that of electrons produced according to the reaction in eq 1. The amount of protons generated during the application of electrical potential to the coated ITO substrate was higher than that of bare ITO substrate, as shown in Figure 8. This can be explained by considering that the electrolysis of water is pushed forward to the product (protons and oxygen) side of the reaction by Le Chatelier's principle as protons are consumed to protonate the COO^- groups of PAA. This hypothesis is in good agreement with FTIR results of the 4(LPEI/PAA)$_{20}$ LbL films that show

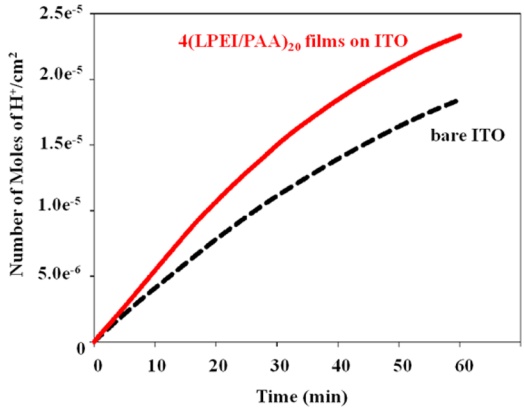

Figure 8. Number of protons generated in the presence of either an ITO substrate or an ITO substrate coated in a LbL film after application of an electric field for various times.

protonation progressing with time. As can be seen in Figure 6b, the degree of ionization of PAA decreased while the reaction of water electrolysis occurs, which means that the COO^- groups of PAA were neutralized by protons produced. Therefore, the continuous consumption of protons can move the reaction forward (toward the H^+ product side of the electrolysis reaction) compared to the case of bare ITO.

CONCLUSIONS

In this report, we use an electric field to manipulate PEMs post assembly. Application of an electric field locally lowers the pH in aqueous solution at the electrode because of the hydrolysis of water. When that electrode is coated with a PEM this local drop in pH can be used to induce a morphological change in the film resulting in a porous structure. Depending on the duration of the application of electrical potential, the multilayers exhibited a range of morphologies. This began with the formation of nonconnected nanoscale pores at the electrode/multilayer interface, then an asymmetric porous structure, and finally connected microsized pores throughout the films. The ability to precisely control the application of potential therefore allows us to control pore structure. This includes the on-demand formation of nano or microscaled features, and closed or open celled morphologies that have not been observed in PEMs with other types of post assembly processing. The variation of pore structure is closely related to the reorganization of polymer chains, resulting from changes in

dx.doi.org/10.1021/am400667y | ACS Appl. Mater. Interfaces 2013, 5, 4930–4936

the chains' charge density. It was also shown that this method can be used to control binding and release of small molecules (MB in this case) within the multilayer environment based on charge density with application of an electric field.

■ ASSOCIATED CONTENT

Supporting Information

Figures S1−S8, which include experiment schematics, photographs of samples, AFM and SEM images, roughness data, and UV−vis data. This material is available free of charge via the Internet at http://pubs.acs.org.

■ AUTHOR INFORMATION

Corresponding Author

*E-mail: nzacharia@tamu.edu. Phone: 1 (979) 845-2204.

Notes

The authors declare no competing financial interest.

■ ACKNOWLEDGMENTS

The authors would like to thank Texas A&M University and the Texas Engineering Experiment Station for startup funds for the support of this work as well as the Texas Space Grant New Investigations Program. The authors also thank Dr. Sreeram Vaddiraju for use of his UV−vis instrument.

■ REFERENCES

(1) Zhu, H.; Ji, J.; Shen, J. *Biomacromolecules* **2004**, *5*, 1933−1939.
(2) Watanabe, J.; Eriguchi, T.; Ishihara, K. *Biomacromolecules* **2002**, *3*, 1375−1383.
(3) Furbert, P.; Lu, F.; Winograd, N.; DeLouise, L. *Langmuir* **2008**, *24*, 2908−2915.
(4) Salehi, P.; Sarazin, P.; Ravis, B. D. *Biomacromolecules* **2008**, *9*, 1131−1138.
(5) Xiang, Z.; Sarazin, P.; Favis, B. D. *Biomacromolecules* **2009**, *10*, 2053−2066.
(6) Lecomte, F.; Siepmann, J.; Walther, M.; MacRae, R. J.; Bodmeier, R. *Biomacromolecules* **2005**, *6*, 2074−2083.
(7) Wang, C.; Wang, Q.; Wang, T. *Langmuir* **2010**, *26*, 18357−183361.
(8) Watanabe, K.; Yuasa, M.; Kida, T.; Shimanoe, K.; Teraoka, Y.; Yamazoe, N. *Chem. Mater.* **2008**, *20*, 6965−6973.
(9) Hess, K. C.; Epting, W. K.; Litster, S. *Anal. Chem.* **2011**, *83*, 9492−9498.
(10) Kuo, C.; Chen, Y.; Lu, S. *ACS Appl. Mater. Interfaces* **2009**, *1*, 72−75.
(11) Joo, W.; Park, M. S.; Kim, J. K. *Langmuir* **2006**, *22*, 7960−7963.
(12) Park, M.S.l; Kim, J. K. *Langmuir* **2005**, *21*, 11404−11408.
(13) Shimomura, H.; Gemici, Z.; Cohen, R. E.; Rubner, M. F. *ACS Appl. Mater. Interfaces* **2010**, *2*, 813−820.
(14) Lee, L. J.; Zeng, C.; Cao, X.; Han, X.; Shen, J.; Xu, G. *Compos. Sci. Technol.* **2005**, *65*, 2344−2363.
(15) Decher, G. *Science* **1997**, *277*, 1232−1237.
(16) Mendelsohn, J. D.; Barrett, C. J.; Chan, V. V.; Pal, A. J.; Mayes, A. M.; Rubner, M. F. *Langmuir* **2000**, *16*, 5017−5023.
(17) Lutkenhaus, J. L.; McEnnis, K.; Hammond, P. T. *Macromolecules* **2008**, *41*, 6047−6054.
(18) Lichter, J. A.; Rubner, M. F. *Langmuir* **2009**, *25*, 7686−7694.
(19) Lowman, G. M.; Tokuhisa, H.; Lutkenhaus, J. L.; Hammond, P. T. *Langmuir* **2004**, *20*, 9791−9795.
(20) Berg, M. C.; Zhai, L.; Cohen, R. E.; Rubner, M. F. *Biomolecules* **2006**, *7*, 357−364.
(21) Cho, C.; Valverde, L.; Ozin, G. A.; Zacharia, N. S. *Langmuir* **2010**, *26* (13637), 13643.
(22) Guo, Z.; Chen, X.; Xin, J.; Wu, D.; Li, J.; Xu, C. *Macromolecules* **2010**, *43*, 9087−9093.
(23) Tian, Y.; Qiang, H.; Cui, Y.; Tao, C.; Li, J. *Chem.—Eur. J.* **2006**, *12*, 4808−4812.
(24) Fu, Y.; Bai, S.; Cui, S.; Qiu, D.; Wang, Z.; Zhang, X.; et al. *Macromolecules* **2002**, *35*, 9451−9458.
(25) Bai, S.; Wang, Z.; Zhang, Z.; Wang, B. *Langmuir* **2004**, *20*, 11828−11832.
(26) Bai, S.; Wang, Z.; Gao, J.; Zhang, X. *Eur. Polym. J.* **2006**, *42*, 900−907.
(27) Zhang, H.; Fu, Y.; Wang, D.; Wang, L.; Wang, Z.; Zhang, X. *Langmuir* **2003**, *19*, 8497−8502.
(28) Cho, C.; Zacharia, N. S. *Langmuir* **2012**, *28*, 841−848.
(29) Glazer, P. J.; van Erp, M.; Embrechts, A.; Lemay, S. G.; Mendes, E. *Soft Matter* **2012**, *8*, 4421−4426.
(30) Van Tassel, P. R. *Curr. Opin. Colloid Interface Sci.* **2012**, *17*, 106−113.
(31) Choi, J.; Rubner, M. F. *Macromolecules* **2005**, *38*, 116−124.
(32) Guillaume-Gentil, O.; Graf, N.; Boulmedais, F.; Schaaf, P.; Voros, J.; Zambelli, T. *Soft Matter* **2010**, *6*, 4246.
(33) Ko, Y. H.; Kim, Y. H.; Park, J.; Nam, K. T.; Park, J. H.; Yoo, P. J. *Macromolecules* **2011**, *44*, 2866−2872.
(34) Schmidt, D.; Min, Y.; Hammond, P. T. *Soft Matter* **2011**, *7*, 6637.
(35) Ladam, G.; Schaad, P.; Voegel, J. C.; Schaaf, P.; Decher, G.; Cuisinier, F. *Langmuir* **2000**, *16*, 1249−1255.
(36) Zacharia, N. S.; DeLongchamp, D. M.; Modestino, M.; Hammond, P. T. *Macromolecules* **2007**, *40*, 1598−1603.
(37) Zacharia, N. S.; Modestino, M.; Hammond, P. T. *Macromolecules* **2007**, *40*, 9523−9528.
(38) Geoffrey, M. L.; Tokuhisa, H.; Lutkenhaus, J. L.; Hammond, P. T. *Langmuir* **2004**, *20*, 9791−9795.
(39) Itano, K.; Choi, J.; Rubner, M. F. *Macromolecules* **2005**, *38*, 3450−3460.
(40) Sui, Z.; Schlenoff, J. B. *Langmuir* **2004**, *20*, 6026−6031.
(41) Lee, J. Y.; Painter, P. C.; Coleman, M. M. *Macromolecules* **1998**, *21*, 346−364.
(42) Elvira, T.; Quinn, J. F.; Caruso, F. *Langmuir* **2005**, *21*, 8785−8792.
(43) Xie, A. F.; Graniks, S. *Macromolecules* **2002**, *35*, 1805−1813.
(44) Li, Q.; Quinn, J. F.; Caruso, F. *Adv. Mater.* **2005**, *17*, 2058.
(45) Heger, D.; Jirkovsky, J.; Klan, P. J. *Phys. Chem. A* **2005**, *109*, 6702−6709.
(46) Parkanyi, C.; Boniface, C.; Aaron, J. J.; Maafi, M. *Spectrochim. Acta, Part A* **1993**, *49*, 1715.
(47) Chung, A. J.; Rubner, M. F. *Langmuir* **2002**, *18* (4), 1176−1183.
(48) Ding, C.; Xu, S.; Wang, J.; Liu, Y.; Hu, X.; Chen, P.; Feng, S. *Polym. Adv. Technol.* **2012**, *23*, 1283−1286.
(49) Kittredge, M. C.; Durst, T. S.; Kittredge, K. W. *Thin Solid Films* **2010**, *518* (14), 3949−3953.
(50) Bergmann, K.; O'Konshk, C.T. J. *Phys. Chem.* **1963**, *67*, 6169.
(51) Braswell, E. J. *Phys. Chem.* **1968**, *72*, 2477.
(52) Ngankam, A. P.; Van Tassel, P. R. *Proc. Natl. Acad. Sci. U.S.A.* **2007**, *104*, 1140.